Effect of the liquid layer on the impact behaviour of particles

S. Antonyuk[1], S. Heinrich[1], M. Dosta[1], M.S. van Buijtenen[2], N.G. Deen[2] and J.A.M. Kuipers[2]

[1] Institute of Solids Process Engineering and Particle Technology, Hamburg University of Technology, Denickestrasse 15, 21071 Hamburg, Germany
[2] Institute for Mechanics Processes and Control Twente, University of Twente, PO Box 217, Enschede, 7500 AE, The Netherlands

Abstract

During a spray granulation process the moisture loading in fluidized beds has a great influence on the inter-particle collision properties and hence on the flow behaviour. To study the influence of the liquid layer as well as granule impact velocity on the impact behaviour free-fall experiments were performed. During these experiments the γ-Al_2O_3 granules were dropped from a predefined height onto a liquid layer on the flat steel wall and the velocity-time curves were obtained using high-speed video recording. The height of the liquid layer was varied from 50 μm to 1 mm. Moreover, the tests were performed at different velocities and viscosities of liquid layer in the range of 1-300 mPa·s. Both distilled water and water solutions of hydroxypropyl methylcellulose with different concentrations (3, 6, 10 mass-%) were used.
The obtained restitution coefficients were compared with the experiments performed without liquid film on the surface. For a granule impacted on a liquid film on the wall, the increase of liquid viscosity decreases the restitution coefficient and thickness of liquid layer at which the granule sticks. In the examined velocity range, with decreasing impact velocity the restitution coefficient greatly decreases. To explain the obtained effects the force and energy balances for a particle impacted on a liquid layer on the wall were derived. Both contributions to energy absorption (granule-liquid layer and granule-wall contacts) have been taken into consideration.

Keywords: Particle Impact, Liquid layer, Liquid bridge, Restitution coefficient, Energy dissipation

1. Introduction

The moisture content in fluidized beds during spray bed granulation or agglomeration has a great influence on the inter-particle collision properties and hence on the flow behavior [1]. During this process the most important mechanisms of particle collisional energy loss are the micro processes of coating of the particle surface with a liquid layer or droplets and the particle wetting [2-3].
The effect of the moisture content on the kinetic energy dissipation during the impact could be significant when the microstructure of the granules becomes softer with wetting, e.g. due to solubility of the material. Therefore, the amount of the plastic deformation increases with moisture content. That was observed for some types of granules in the works [1-3]. However, the influence of the moisture can be minimal for insoluble materials, e.g. the ceramic and zeolite granules [3].
During injection of a liquid binder in the granulator the liquid films and small droplets on the surface of solid particles are formed. These could form liquid bridges during the impact and may lead to sticking of the particles, i.e. agglomeration occurs. The initial kinetic impact energy is dissipated due to shear flow of the liquid between particles during incidence, extension and rupture of a liquid bridge during the rebound [3].
In this work, we study the effects of the thickness and viscosity of the liquid layer as well as granule impact velocity on the energy dissipation during normal impact of a spherical granule on the wall with a liquid layer. Based on the measurements and simulations the influence of these parameters on liquid layer height at which the granule sticks was obtained.

2. Force and energy balances of the particle impact with a liquid layer

The full period of the impact can be divided into four intervals, Figure 1. In the first period, the particle penetrates into the liquid layer and displaces the liquid from contact area. The particle-wall contact with a total displacement x_{tot} takes place during the second period. After loss of the contact the particle moves upward through the liquid up to the liquid layer surface (the third period). During the last period a liquid bridge is formed. This bridge will be stretched up to a critical length $h_{br,max}$ where its rupture occurs.

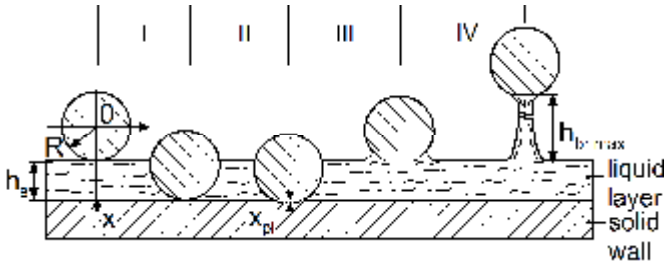

I. Particle penetration: $x \downarrow \in [0;\ h_s]$

II. Granule-wall contact: $x \downarrow \in [h_s;\ h_s+x_{tot}]\ \uparrow[h_s+x_{tot};\ h_s+x_{pl}]$

III. Emergence of particle: $x \uparrow \in [h_s;\ 0]$

IV. Formation of the liquid bridge: $x \uparrow \in [0;\ -h_{br,max}]$

Figure 1. Schematic representation of impact intervals.

The equation of motion of a particle impacted on the wall with a liquid layer could be expressed as:

$$m_p \frac{d^2\mathbf{x}}{dt^2} = \mathbf{F}_{p,g} + \mathbf{F}_t + \mathbf{F}_b + \mathbf{F}_D + \mathbf{F}_c + \mathbf{F}_{vis} + \mathbf{F}_{cap} + \mathbf{F}_{l,g}, \qquad \text{Eq (1)}$$

where x is the vertical position of the particle centre, i.e. the particle displacement. The forces acting on the particle during impact and rebound (Figure 2) are: $F_{p,g}$, $F_{l,g}$ - gravitational forces of the particle and the liquid film on the particle, F_t - surface tension force, F_b - buoyancy force, F_D - drag force, F_c - contact force between the particle and the wall, F_{vis} - viscous force, F_{cap}- capillary force.

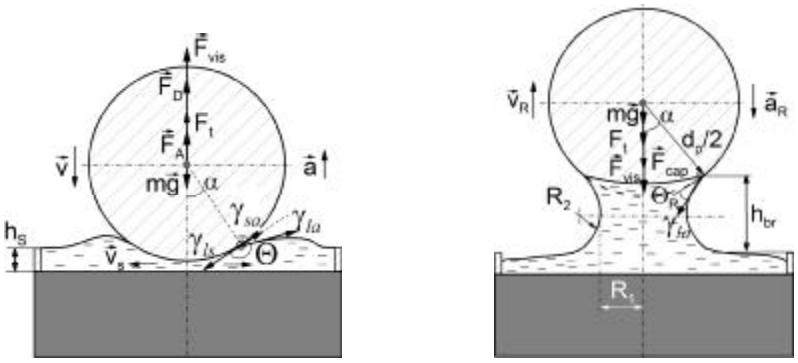

I - penetration IV - rebound (liquid bridge)

Figure 2. Forces acting on the particle during the penetration and rebound.

The surface tension force F_t was determined for a liquid bridge under static conditions by Orr et al. [4], calculated and measured by many authors [5, 6] as:

$$F_t = \pm\gamma_{la}\ \pi\, d_p\ \sin\alpha \sin(\Theta+\alpha), \qquad \text{Eq (2)}$$

where g_{la} is the liquid-air surface tension and α is a half of central angle (Figure 2). The dynamic contact angle Θ depends on the wetting conditions of the particle. It can be greater than 90° during

the penetration (i.e. particle wetting) and less than 90° during the rebound (i.e. pull-back of the liquid from the surface).
The capillary force in the liquid bridge depends on the Laplace hydrostatic pressure difference across the fluid surface and on the cross-section area of the neck:

$$F_{cap} = -\Delta p A_D = -\gamma_{la}\left(\frac{1}{R_1} - \frac{1}{R_2}\right)\pi R_p^2 \sin^2\alpha \,. \qquad \text{Eq (3)}$$

where R_1 and R_2 are the local radii of the curvature (Figure 2). Here a minus is written before the radius R_2 due to concave meridional curvature of the bridge.
The total force on the particle in the static state results from the sum of capillary and tensile forces. Figure 3 shows the well-know dimensionless representation of the total force related to surface tension and particle diameter versus the ratio of separation distance h_s to particle diameter d_p, calculated and measured by Schubert [5]. The force decreases with separation distance, and this decreasing is stronger for smaller ratio of liquid to solid volume, i.e. for thinner bridges.

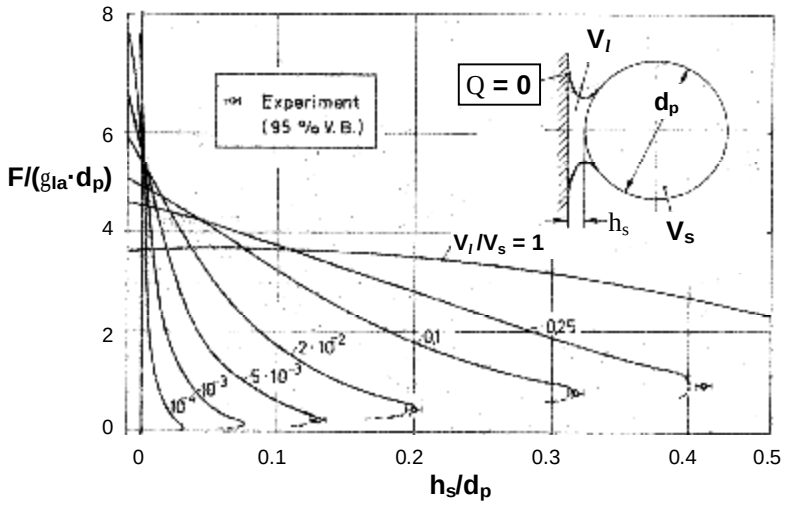

Figure 3. Force acting on the particle with a liquid bridge at a static loading.

In investigated cases the buoyancy force is relative small and can be neglected. The drag force F_D can be calculated by the following equation:

$$F_D = \pm\frac{1}{8}\pi c_D \rho_l d_p^2 \sin^2\alpha \, v^2, \qquad \text{Eq (4)}$$

where v is the particle velocity and c_D is the drag coefficient which is according to Kaskas [7]:

$$c_D = 24/\mathrm{Re} + 4/\sqrt{\mathrm{Re}} + 0.4 \qquad \text{Eq (5)}$$

for the Reynolds number range: $0 < Re < (2\text{-}4)\cdot 10^5$.
During the second period of the impact the granule-wall contact takes place. The contact force F_c can be expressed as a sum of an elastic force (first term in Eq. (6) according to Hertz) and a damping force (second term in Eq. (6) according to Tsuji [8]):

$$F_c = k'_{el} x_c^{3/2} + \alpha_d \sqrt{m^* k'_{el}}\, x_c^{1/4} \frac{dx_c}{dt}, \qquad \text{Eq (6)}$$

with the contact displacement x_c, median radius $R^* = (1/R_p + 1/R_w)^{-1} \approx R_p$ and effective mass $m^* = (1/m_p + 1/m_w)^{-1} \approx m_p$ of contact partners. Note that we use index p for the particle and index w for the wall. The effective modulus of elasticity E^* of impacting bodies ($E_w >> E_p$, $E_w \to \infty$) is given as:

$$E^* = 2\left(\frac{1-\nu_p^2}{E_p}+\frac{1-\nu_w^2}{E_w}\right)^{-1} \approx \frac{2E_p}{1-\nu_p^2}, \qquad \text{Eq (7)}$$

where ν is the Poisson ratio.
The Hertzian constant k'_{el} in Eq. (6) can be given by the following expression:

$$k'_{el} = \frac{2}{3}E^*\sqrt{R^*}. \qquad \text{Eq (8)}$$

The energy dissipation in the contact model is controlled by a damping parameter α_d which depends on the restitution coefficient. The restitution coefficient and Hertzian constant can be obtained experimentally using compression or free-fall tests [9].
The viscous resistance arises during particle movement in the liquid due to the liquid shear flow between granule and wall. For a Newtonian fluid the viscous force was found as [10], [11]:

$$F_{vis} = \pm\frac{6\,\pi\,\eta\,R_p^2}{h_s - x}\frac{dx}{dt}, \qquad \text{Eq (9)}$$

where h is the viscosity of the liquid and (h_s-x) is the separation distance between particle and wall surfaces (Figure 1).
The gravitation force $F_{l,g}$ in Eq. (1) considers the mass of a liquid film which moves with the particle in the last period of impact.
The energy loss $E_{diss,tot}$ during particle collisions can be described using the restitution coefficient which is equal to the square root of the ratio of elastic energy $E_{kin,R}$ released during the restitution to the initial kinetic impact energy E_{kin}:

$$e = \sqrt{\frac{E_{kin,R}}{E_{kin}}} = \sqrt{1-\frac{E_{diss,tot}}{E_{kin}}} = \frac{|v_R|}{v}, \qquad \text{Eq (10)}$$

where E_{kin} is an energy on the liquid layer height (x = 0 in Figure 1) and $E_{kin,R}$ is related to the bridge cut height (x = - $h_{br,max}$).
The energy balance for the impacted particle can be expressed in general form as follows:

$$E_{kin} = E_{kin,R} + E_{diss,tot}\left(\sum F_{diss}\right) + \Delta E_{mgh,br}, \qquad \text{Eq (11)}$$

where E_{mgh} is the increment of gravitational potential energy of the particle by lifting from liquid level to liquid bridge cut height.

3. Testing method and material

Figure 4 illustrates the used experimental free-fall setup. Before the granule is dropped, it is being held at a predetermined height h above the target (steel flat wall) with the aid of a vacuum nozzle that releases the granule with zero initial velocity and rotation.
The restitution coefficient is a ratio of relative rebound velocity v_R (at the bridge rupture) to that before the impact v (at the contact with the liquid). These velocities were determined from impacts captured using with a high-speed video camera with a frequency of 4.000 fps.
The current value of the thickness was controlled by weighting of the liquid with the help of a precision balance on which the target was placed. The measurement error of the balance was less than 10 mg that corresponds to an error of 5 µm in the layer height.
As test material the spherical elastic-plastic γ-Al_2O_3 granules with smooth surface produced by company SASOL were chosen (Figure 5). The properties of these granules are given in Table 1 [9], [13].

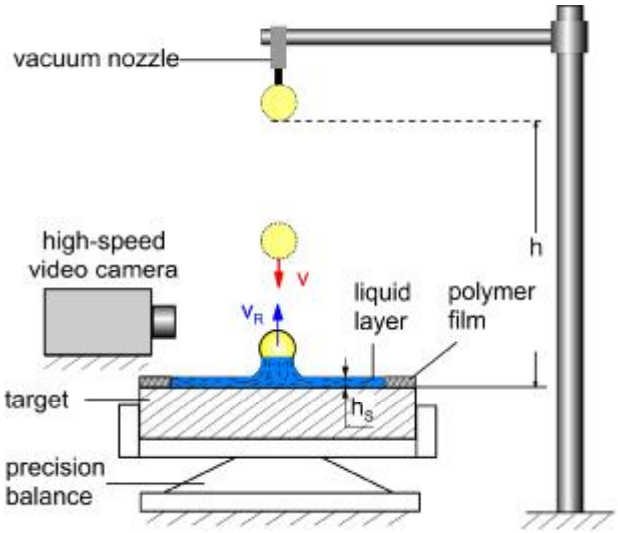

Figure 4. The free-fall device for measurements of granule impact on a wall with a liquid layer.

Property	**Value**
granule size d_p in mm	1.75 ± 0.05
granule density in kg/m^3	1040 ± 6.1
modulus of elasticity E_p in kN/mm^2	14.62 ± 0.3
Hertzian constant k'_{el} in MN/m$^{1.5}$	592 ± 40
Normal restitution coefficient e_n for the impact on the dry steel flat target (at the velocities v = 0.5 – 4.5 m/s)	0.735 ± 0.018

Table 1 Characteristics of the examined granules.

Figure 5. Digital image of examined γ-Al_2O_3 granules.

A polymer film attached to the wall surface forms the borders for the liquid layer. The impact behavior was studied by varying layer thickness from 50 µm to 1 mm. As a liquid medium a water solution of hydroxypropyl methylcellulose Pharmacoat® 606 was used. The concentration of the binder in the solution was varied from 3 to 10 mass-% to study the influence of viscosity in the range of 1-300 mPas. The measurements were carried out at two impact velocities of 1.0 m/s and 2.4 m/s. To increase the statistical significance of the experiment we repeated the free-fall test for each viscosity and height of the liquid 50 times.

4. Data processing

The images from high-speed recording in Figure 6 show the impact of the granule on the liquid surface, the penetration into liquid layer, the formation of a liquid bridge during rebound and its rupture at a critical height. At the beginning the liquid bridge has a symmetrical shape, which can be approximated with two radii of curvature. After time of 3.13 ms the bridge becomes asymmetrical with thinning from bottom to top.

The velocity of the granule was determined from captured impacts using self programmed software on the basis of Matlab. The typical velocity-displacement curves for experiments with and without the liquid layer are shown in Figure 7.

For impacts without a liquid layer the rebound velocity is approximately constant in the range of some millimeters of the displacement. In presence of a liquid bridge the velocity decreases sharply

during the rebound. Therefore, to calculate the restitution coefficient, the rebound velocity is approximated on the short displacement part after the rupture of the liquid bridge.

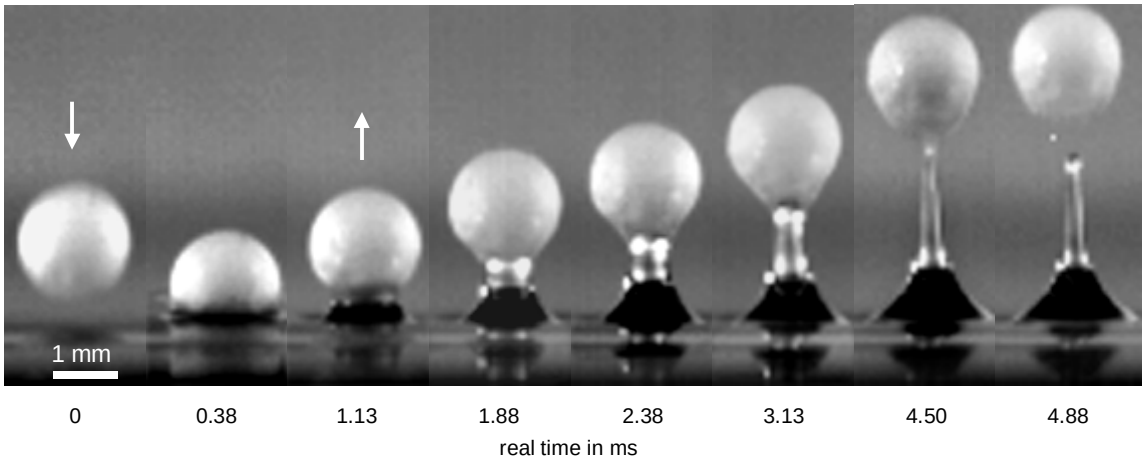

Figure 6. Images from high-speed recording of a γ-Al_2O_3-granule impacted at the velocity of 2.36 m/s on the wall with a water layer (thickness of 400 μm).

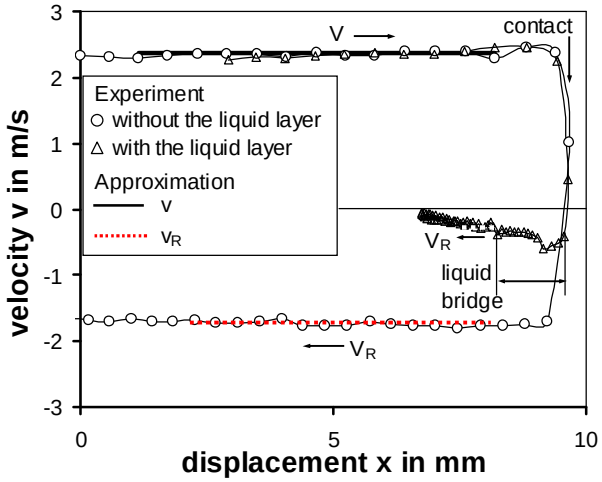

Figure 7. Approximation of the granule velocity before and after impact for typical velocity-displacement curves measured without a liquid layer and with a water layer of 700 μm.

5. Experimental results

The results of free-fall tests are shown in Figure 8. The restitution coefficient becomes smaller with increasing thickness and viscosity of the liquid layer, when the amount of the energy absorption by adhesion increases. The maximum of the restitution coefficient corresponds to the impact without the liquid layer [13]. The minimum of the restitution coefficient equals to zero, i.e. the granule sticks. The corresponding layer thickness h_{st} depends on the viscosity and the impact velocity. With larger binder viscosity this sticking thickness decreases, in Figure 9. Thus, to increase the agglomeration rate of particles, either the viscosity or the thickness of the binder layer should be increased.

The experimental results showed that the decrease of the impact velocity can greatly reduce the restitution coefficient and the sticking height (Figure 10). Therefore, a smaller restitution coefficient is caused by the longer time for energy absorption during penetration in the layer and stretching of the bridge. In contrast to wet conditions, the restitution coefficient of γ-Al_2O_3 granules for the impact without a liquid layer is independent of the velocity in the range of 0.5-4.5 m/s [13].

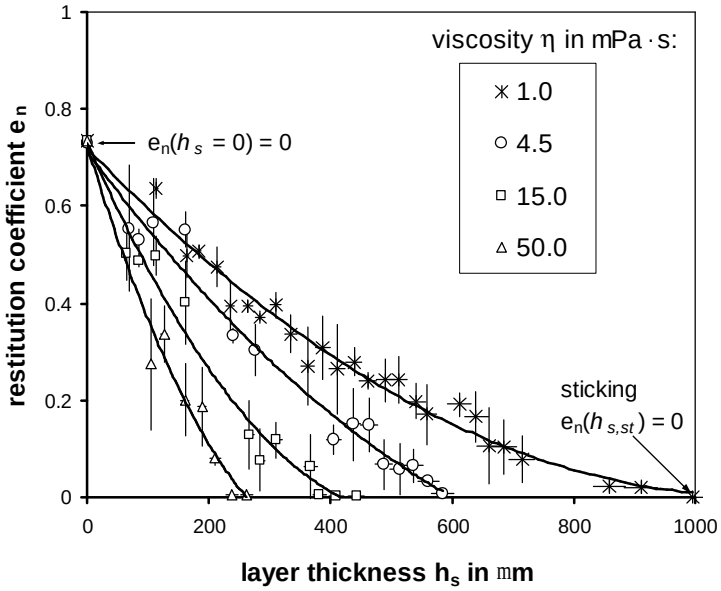

Figure 8. Influence of viscosity *h* and thickness h_s of the liquid layer on restitution coefficient e_n (v = 2.36 m/s).

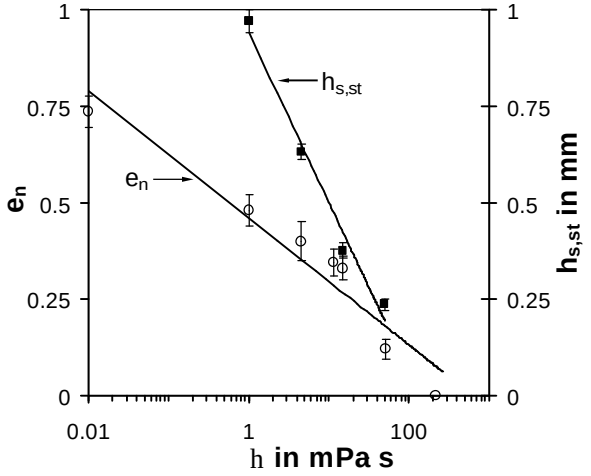

Figure 9. Effect of liquid viscosity on the restitution coefficient e_n of γ-Al_2O_3 granules (layer thickness of 200 μm) and on the sticking thickness h_{st}.

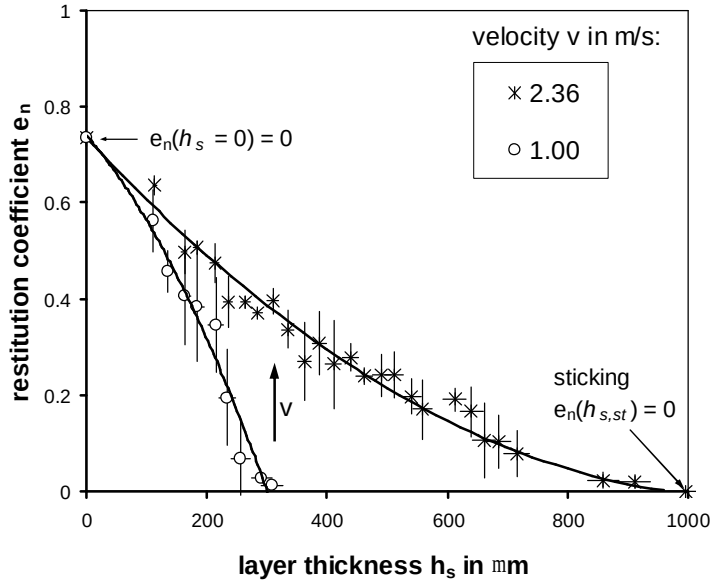

Figure 10. Influence of the impact velocity on restitution coefficient of γ-Al_2O_3 granules impacting on the water layer.

6. Simulation results

The numerical calculations of the equation of motion (1) were performed for the particle impact velocity of 2.36 m/s and the viscosity of h = 4.5 mPa·s which correspond to the conditions of the performed free-fall experiments. The properties of the granules and the liquid were used as material parameters of the model. The damping parameter α_d in model of Tsuji was assumed to be 0.23 according to the "dry" restitution coefficient (e_n = 0.735).
The diagram in Figure 11 compares the experimental obtained and calculated restitution coefficients at different liquid layer thicknesses. A good agreement of the calculated values with experimental data was obtained, however the curve from the simulation is convex while the measured curve is concave, i.e. the effect of the height decreases with the liquid thickness.

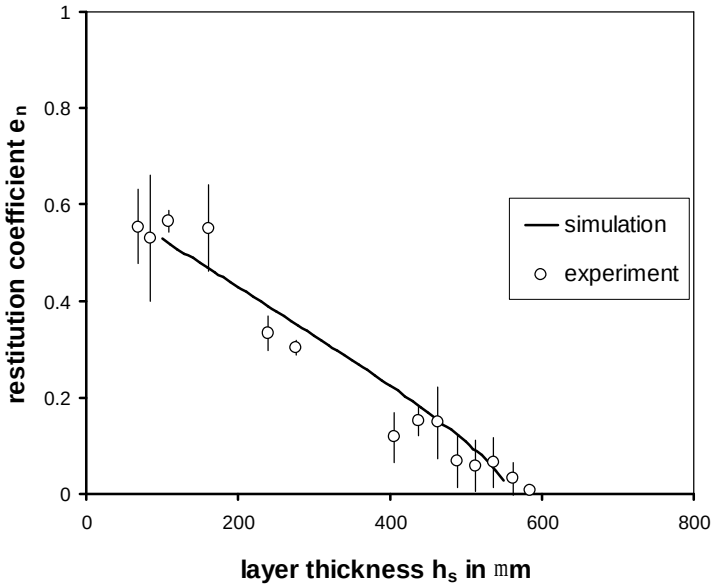

Figure 11. Experimental and calculated normal restitution coefficients versus liquid layer thickness (h = 4.5 mPa·s, g_{la} = 43.6 mN/m and v = 2.36 m/s).

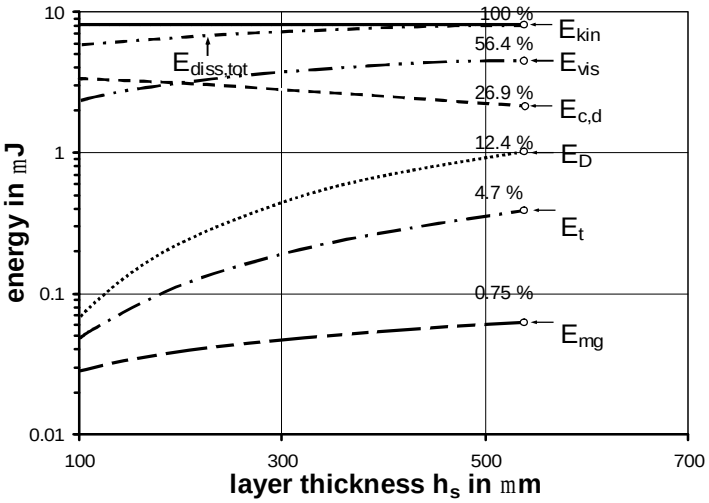

Figure 12. Kinetic impact energy (v = 2.36 m/s) and dissipated energy parts versus liquid layer thickness (h =4.5 mPa·s). The plotted values show the contribution of different energies at the sticking point.

Figure 12 shows the influence of different forces on the total energy dissipation $E_{diss,tot}$ which increases with the layer thickness and arrives the initial kinetic energy E_{kin} at the sticking point. The most important influence on the energy absorption during the penetration and rebound are caused

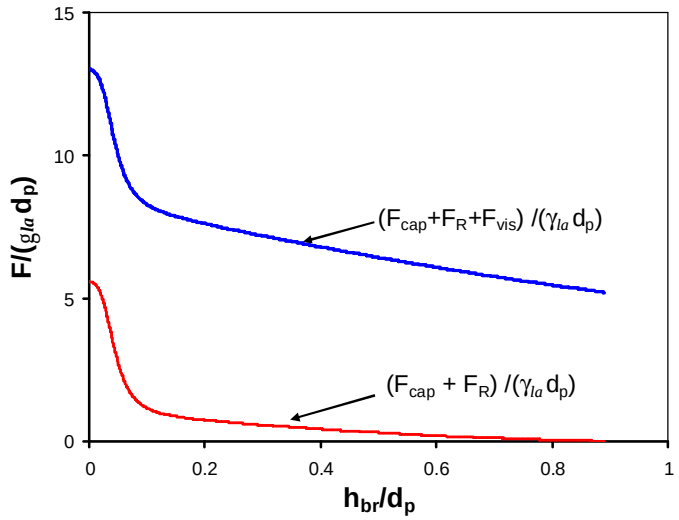

Figure 13. Comparison of the forces acting on the γ-Al_2O_3 granule (d_p = 1.75 mm) with the liquid bridge (h = 4.5 mPa·s, g_{la} = 43.6 mN/m) at static and dynamic conditions (v = 2.36 m/s).

by the viscous (E_{vis}) and contact damping ($E_{c,d}$) forces. The drag force becomes a significant effect only at the thick layers ($h_s/R_p > 0.3$). The surface tension (E_t) should be considered only in static case when the contribution of the drag and viscous forces become smaller. The difference between the static and dynamic forces acting on the particle with a liquid bridge can be obtained from the comparison in Figure 13. The liquid bridge rupture height obtained in the performed experiments is greater than with the calculation of Schubert (Figure 3). For layers with a thickness from 250 µm to 500 µm the rupture height was in the range of 1.4-2.5 mm which equals to the dimension of (0.8-1.4)·d_p.

7. Conclusions

An experimental study of the energy absorption and numerical calculations of the force balance for the granule impact on a stiff wall with a liquid layer have been performed. The results can be summarized as follows:

1. The higher the viscosity and thickness of the liquid layer the more energy dissipates during the impact and the smaller is the critical thickness needed for the sticking of the granule. This parameter may be bigger to enhance the agglomeration rate in a particle granulation process.
2. The restitution coefficient is reduced greatly with decreasing impact velocity. Thus, to simulate the spray agglomeration the neglect of the influence of the impact velocity can lead to a significant error in the prediction of the sticking condition.
3. Based on the equation of motion of a granule impacted on the liquid layer the energy balance was numerically calculated. It is shown that all four collision intervals play an important role in the energy absorption. The contributions of viscous, contact and drag forces to energy dissipation are of great importance.

8. Acknowledgements

The authors grateful acknowledge to the Institute of Electric Power Systems and Institute of Experimental Physics of Otto-von-Guericke-University of Magdeburg for the rent of the high-speed cameras used in this study. We also thank N. Vorhauer and K. Mecke for their help during performing of the experiments.

9. References

1. Fu, J., Adams, M.J., Reynolds, G.K., Salman, A.D., Hounslow, M.J., 2004. Impact deformation and rebound of wet granules. Powder Technology 140, 248-257.

2. Mangwandi, C., Cheong, Y.S., Adams, M.J., Hounslow, M.J., Salman, A.D., 2007. The coefficient of restitution of different representative types of granules. Chemical Engineering Science 62, 437-450.

3. Müller, P., Antonyuk, S., Tomas, J., Heinrich, S., 2008. Investigations of the restitution coefficient of granules. In Bertram, A. and Tomas J. (Eds.) Micro-Macro-Interactions in Structured Media and Particle Systems, 235-243, Springer, Berlin Heidelberg.

4. Orr, F.M., Scriven, L.E., Rivas, P., 1975. Pendular rings between solids: meniscus properties and capillary force. J. Fluid Mech. 67, 723-742.

5. Schubert, H., 1984. Capillary forces - modeling and application in particulate technology. Powder Technology 37, 105-116.

6. Willet, C.D., Adams, M.J., Johnson, S.A., Seville, J.P.K., 2003. Effects of wetting hysteresis on pendular liquid bridges between rigid spheres. Powder Technology 130, 63-69.

7. Kaskas, A.A., 1970. Schwarmgeschwindigkeit in Mehrkornsuspensionen am Beispiel der Sedimentation. Doctoral dissertation, Technical University of Berlin.

8. Tsuji, Y., Tanaka, T., Ishida, T., 1992. Lagrangian numerical simulation of plug flow of cohesionless particles in a horizontal pipe. Powder Technology 71, 239-250.

9. Antonyuk, S., 2006. Deformations- und Bruchverhalten von kugelförmigen Granulaten bei Druck- und Stoßbeanspruchung. Doctoral dissertation, University of Magdeburg, Docupoint Publishers.

10. Cameron, A., 1981. Basis lubrication theory. Ellis Harwood, Chichester.

11. Lian G., Xu, Y., Huang, W., Adams, M.J., 2001. On the squeeze flow of a power-law fluid between rigid spheres. J. Non-Newtonian Fluid Mech. 100, 151-164.

12. Antonyuk, S., Khanal, M., Tomas, J., Heinrich, S., Mörl L., 2006. Impact breakage of spherical granules: experimental study and DEM simulation. Chemical Engineering and Processing 45, 838-856.

13. Antonyuk, S., Heinrich, S., Tomas, J., Deen, N. G., van Buijtenen, M.S. and J. A. M. Kuipers. Energy absorption during compression and impact of dry elastic-plastic spherical granules, Submitted in Granular Matter, 2009.